1 Introduction

The scope and magnitude of future changes to Earth's climate is of paramount concern for humanity. Changes in land and ocean temperatures, shifting patterns of precipitation, increased frequency of droughts and floods, and melting snow and ice will all have profound impacts – on global food security (*Battisti and Naylor*, 2009), water resource availability (*Oki and Kanae*, 2006), ecosystems (*Deutsch et al.*, 2008) and coastal communities (*Nichols and Cazenave*, 2010). Present day policy decisions and adaptation planning hinge critically on both the anticipated magnitude and spatial patterns of future climate change.

There is a scientific consensus on the large-scale spatial pattern of climate change (e.g. the Arctic will warm more than the tropics (*Holland and Bitz*, 2003), wet places will moisten and dry will become drier (*Held and Soden*, 2006) the tropics will expand (*Lu et al.*, 2007) and the mid-latitude jet stream will shift poleward (*Yin*, 2005)). These patterns are robust because we understand the basic physical processes that lead to these changes, and they are well represented (and relatively consistent between) state of the art climate models (*Taylor et al.*, 2012). In contrast, the magnitude of global mean temperature increase for a given greenhouse forcing – often summarized in terms of the *climate sensitivity* (CS)– is highly uncertain: CS differs by a factor of three across climate models (*Forster et al.*, 2013) and is constrained only to about a factor of four when estimated from observations (*Marvel et al.*, 2015). Within the models, the uncertainty in CS arises mainly from difficulties in simulating how clouds will change with warming; from observations, uncertainty in CS arises mainly from the large uncertainty in historical radiative forcing (*Armour and Roe*, 2011). Despite enormous international efforts, the large inter-model spread in CS has not decreased appreciably over the last several decades (*Stocker et al.*, 2013).

Predicting and planning for future climate change requires understanding where the CS of Earth falls relative to the array of GCM simulated responses to external forcing; should we expect the Earth to warm as much as the mean of the all the model simulations? Might future warming lie outside the range in CS that GCMs predict? Reducing the uncertainty in CS requires either: 1. improvement of model representation of critical processes such that global climate models (GCMs) converge on the estimate of CS or 2. using observational constraints to inform where Earth's climate system falls within the spectrum of CS in GCMs. In the proposed work, we take the latter approach; we propose a novel methodology that uses the relatively short satellite record of top of atmosphere (TOA) radiation to extract information about Earth's radiative response to surface temperature changes and, in turn, the climate sensitivity

Instead of attempting to reduce the GCM spread in CS, we *take advantage of the inter-model spread in CS to ask how the month-to-month variability of global mean radiative imbalance in GCMs informs the CS in the same model.* The goal is to develop a robust method for calculating CS from the existing observational data (satellite radiation from CERES and surface temperature) only. To develop this methodology, we will use the full suite of coupled GCMs where simulations of the month-to-month variability over the historical record – akin to the available observational data – and the long-term response to climate forcing (i.e. the CS) are both available. We will use the combination of the SHORT (month-to-month) and LONG (response to greenhouse forcing) simulations to ask: how can we use limited length records of month-to-month variability to produce

unbiased estimates long-term CS? We will then use the optimal methodology for estimating CS from short term variability to produce an improved observational estimate of CS.

The diversity of climate sensitivities in the GCM ensemble will allow us to hone our methodology for extracting the physics responsible for the long-term CS from month-to-month variability. We can also ask how the estimation of CS would be improved by the prolongation of existing observational platforms, increased accuracy and spatio-temporal resolution of measurements and additional observed fields. In this sense, we will use subsets of the GCM output as observing system simulation experiments to ask how much estimates of CS would benefit from enhanced and prolonged observations.

2 The challenge of estimating climate sensitivity from observations

Global warming is fundamentally caused by energy accumulation in the climate system as a result of a TOA radiative anomaly (RAD_{TOA}) that has been driven by radiative forcing. The vast majority of the energy imbalance is stored in the ocean (*Rhein et al.*, 2013) resulting in a near balance of RAD_{TOA} and the tendency in ocean heat content (OHC). Ultimately, the global mean surface temperature change (T_S) resulting from a given forcing (F) is determined by the climate feedback parameter (λ – units of W m^{-2} K^{-1}) which is a measure of how efficiently the system radiates excess energy to space per degree change in T_S. Earth's energy budget at any given time can this be approximated as:

$$RAD_{TOA} = F + \lambda T_S + \eta_{RAD} \approx d(OHC)/dt, \tag{1}$$

where η_{RAD} is the radiative noise or, more generally, the portion of RAD_{TOA} that is not explained by external forcing (F) or the radiative feedback response to surface temperature changes (λT_S). We emphasize here that much of the radiative variability –especially at shorter time scales– is unrelated to either forcing (F) or surface temperature feedbacks (λ T_S) and the framework developed in the proposed work will explicitly analyze the impact of these other radiative processes (encompassed in η_{RAD}) on estimates of climate feedbacks (λ). In response to a sustained forcing, equilibrium is achieved when $\mathrm{RAD}_{TOA} \rightarrow 0$ at which point the equilibrium surface temperature change (T_{EQ}) of

$$T_{EQ} = -F/\lambda. \tag{2}$$

Note that λ is defined as negative when energy is lost at the TOA as T_S increases, as would be expected of the Planck feedback. Formally, we can define CS as the equilibrium surface temperature response caused by a doubling of atmospheric CO_2 concentration so that

$$CS = F_{2\times CO_2}/-\lambda, \tag{3}$$

where the radiative forcing, $F_{2\times CO_2}$ is typically taken to be around 3.7 w m^{-2} (*Myhre et al.*, 1998) per CO_2 doubling. CS is inversely proportional to λ because a system that is more efficient at exporting energy to space with warming (more negative λ value) requires a smaller T_{EQ} for a given forcing. λ encompasses many different climate feedbacks – defined as the TOA radiative anomaly due to changes in the properties of the climate system that accompany the surface warming. These include the Planck feedback (the change in outgoing longwave radiation that directly results from

a vertically uniform warming of the surface and atmospheric column); the water vapor feedback (atmospheric moistening); the surface albedo feedback (changes in snowpack, sea ice and vegetation); the lapse rate feedback (changes in the thermal structure of the atmosphere); and the cloud feedback (*Bony et al.*, 2006).

The two major strategies for determining λ and, hence, climate sensitivity from modern observational data are:

- **1.)** Using estimates of global surface temperature changes, climate forcing, and energy accumulation in the climate system (i.e. RAD_{TOA} based on observed changes in OHC) to determine climate feedbacks based on the global energy balance described by Eq. 1 (*Forster and Taylor*, 2006):$\lambda = \frac{F - RAD_{TOA}}{T_S}$.
- **2.)** Use of an "emergent" constraint whereby the correlation between (the inter-model spread of) a variable in historical model simulations and that model's CS can be used in conjunction with observations of that variable to give an estimate of Earth's CS (e.g *Fasullo and Trenberth*, 2012; *Sherwood et al.*, 2014; *Marvel et al.*, 2015)

There are potential problems with the two methods identified by number above: 1.) Satellite measurements of RAD_{TOA} have large (≈ 5 W m^{-2}) absolute errors (*Loeb et al.*, 2009) and, therefore, there are no direct measurements of either the TOA radiative imbalance or the climate forcing. As a result, calculation of λ via method 1 estimates RAD_{TOA} indirectly from changes in OHC and radiative forcing from estimates of emissions and the radiative impact of atmospheric constituents. Both quantities have significant uncertainties due to unknown aerosol emissions (*Myhre et al.*, 2013), the "effective forcing" of each atmospheric constituent (*Sherwood et al.*, 2014) and the sparseness of ocean heat content measurements (*Antonov et al.*, 1998). 2.) Given that there is no *a priori* physical relationship between emergent constraint variables and CS, it is possible that the correlation with CS has no physical basis and results simply by chance given the immense number of variables exported by climate models (*Caldwell et al.*, 2015) and, therefore, does not provide an observational constraint on Earth's climate sensitivity. As a result of these methodological and observational uncertainties, current observational estimates of CS differ by a factor of four and are even larger than the inter-GCM spread in CS (*Marvel et al.*, 2015). Furthermore, both of these estimates do not make use of the satellite observations due to the relatively large absolute errors in RAD_{TOA} measured by satellites (≈ 5 W m^{-2}) .

An alternative approach is to estimate how efficiently energy is exported from the climate system to the TOA as the surface warms (thus giving an estimate of λ) using the covariance of the monthly or inter-annual variability of RAD_{TOA} and T_S over the relatively short satellite record. The underlying assumption of this approach is that λ captures the fundamental physics of how much energy gets lost to space as the surface warms and that those physics are independent of timescale. That is, one unit of T_S change will result in the same magnitude change in the radiation emitted to space (equal to λT_S) regardless of whether the temperature change (T_S) resulted from internal variability or radiative forcing. The simplest estimate of λ is then given by the regression coefficient between (forcing removed) RAD_{TOA} anomalies and T_S (Fig. 1C) which we will refer to as λ_{SHORT}. This method has been widely used in the literature (*Donohoe et al.*, 2014; *Murphy et al.*, 2009; *Trenberth et al.*, 2015; *Tsushima et al.*, 2005; *Dessler*, 2013; *Forster and Taylor*, 2006; *Chung et al.*, 2010; *Trenberth et al.*, 2010), with the further assumption that the estimated λ can be used to constrain CS via Eq. 3. However, these assumptions are only valid in the limits that (i) η_{RAD} in Eq. 1 is uncorrelated with T_S, so that λ can be estimated from linear regression analysis; and (ii) the same λ that applies at month-to-month or inter-annual timescales also applies at long

timescales. As we will show here, neither of these assumptions are valid.

We present two lines of evidence that this method is erroneous for predicting long-term climate feedbacks (λ_{LONG}) and, hence, CS: 1. λ_{SHORT} is highly sensitive to the timescale of variability (*Forster*, 2015) and 2. when applied to month-to-month variability in climate model simulations, the calculated λ_{SHORT} does not match the λ_{LONG} diagnosed from the simulated response to greenhouse forcing (*Chung et al.*, 2010) in the same model. We present and expand on this evidence below.

- **Timescale dependence of λ_{SHORT} in observations (Fig. 1).** The nearly 16 years of RAD_{TOA} data from the Clouds and Earth's Radiant Energy System (CERES *Wielicki et al.*, 1996) experiment in conjunction with T_S variability allows one to calculate λ_{SHORT} from the regression coefficient between RAD_{TOA} (with greenhouse gas forcing trends removed) and T_S (*Donohoe et al.*, 2014). Monthly anomalies in RAD_{TOA} are weakly (R=0.25) but significantly (99% confidence interval) correlated with T_S (open dots in Fig. 1C) with a regression slope of -1.4 $\pm$0.4 W m^{-2} K^{-1} implying a CS (2.6K) close to the middle of the IPCC model range. However, if annual mean data are used (shaded squares in Fig. 1C), the regression slope is -3.0 $\pm$ W m^{-2} K^{-1} which implies a CS that is much lower (1.2 K) and one that is lower than the IPCC model range. The sensitivity of λ_{SHORT} to averaging timescale is demonstrated by the purple dots in Fig. 1D by applying a low pass filter with varying cutoff period to the CERES data prior to calculating λ_{SHORT} via regression; λ_{SHORT} varies by a factor of 3 across averaging timescale with largest climate sensitivities found for both the monthly and 5 year variability and smallest sensitivities found for 2-3 year averaging. We emphasize that the implicit assumptions underlying the calculation of CS from the regression of RAD_{TOA} against T_S would predict that λ_{SHORT} is time invariant and isolates the radiative feedbacks responsible for the long-term adjustment of the climate system. Clearly, non-feedback radiative processes are influencing the calculation of λ_{SHORT}. Furthermore, while it may seem intuitive that longer averaging periods lead to more reliable estimation of λ_{LONG}, without understanding the physical processes responsible for the dependence of λ_{SHORT} on timescale, it is unclear if the annual mean calculation or the monthly calculation is more reliable for isolating radiative feedbacks (*Forster*, 2015).
- **Discrepancy between λ_{SHORT} and λ_{LONG} in GCMs (Fig. 2).** To address the question of whether λ_{SHORT} calculated from short-term variability isolates the physical processes that determine CS (i.e. λ_{LONG}), we turn to the CMIP5 suite of coupled climate models for guidance. In particular, we compare two quantities that are each calculated in the same climate model: **1.** λ_{SHORT} calculated as the regression coefficient between global and annual mean T_S and RAD_{TOA} anomalies in a 500 year long unforced pre-industrial (PI) simulation and **2.** λ_{LONG} calculated in response to an instantaneous CO_2 quadrupling ($4XCO_2$) as the linear best fit between RAD_{TOA} and T_S after the forcing has been applied (*Gregory and Webb*, 2008). λ_{SHORT} is not equal to and is poorly correlated with λ_{LONG} in the CMIP5 ensemble (Fig.2); the models (colored dots) fall fairly far from the black diagonal 1:1 line. There is no significant correlation (R=-0.16) between the inter-model spread in λ_{SHORT} and λ_{LONG} (as was previously reported by *Chung et al.*, 2010). This result suggests that simply taking the covariance between RAD_{TOA} and T_S from internal variability provides no constraint on the CS. Furthermore, the majority of models calculate a smaller magnitude λ from inter-annual variability as compared to that from external forcing (most models fall to the right of 1:1 line) implying that CS deduced from inter-annual variability is biased high. We further note

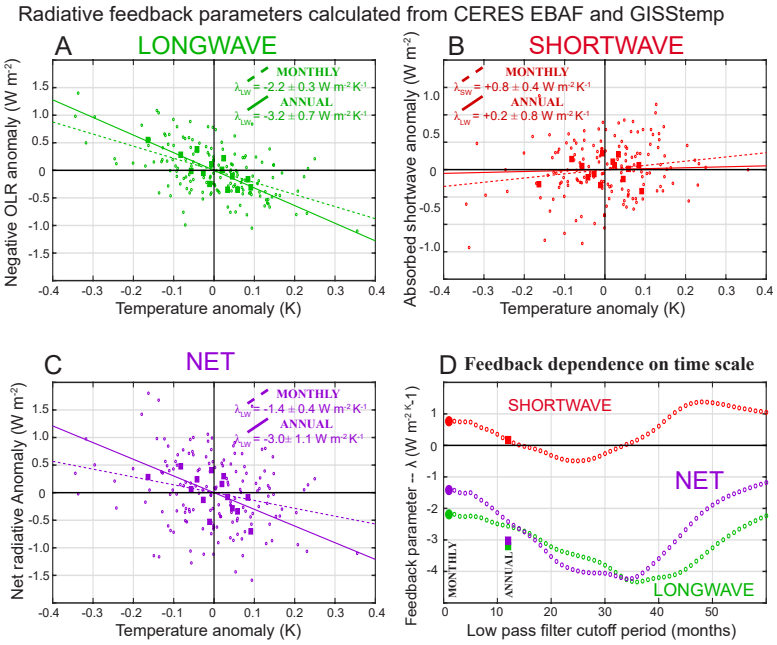

Figure 1: (A-C) Scatter plot of global mean anomalies in TOA radiation (positive into the Earth) versus global mean surface temperature anomaly. Monthly means are shown by hollow circles – with linear best fit shown by dashed lines– and shaded squares are the annual means – with solid line showing the linear best fit. Panel A shows the longwave, panel B the shortwave and panel C the net radiation. Radiative data are from CERES with radiative forcing removed. Temperature data are from GISSTEMP (*Hansen et al.*, 1999). (D) The feedback parameters resulting from low pass filtering the monthly data with cutoff period given by the abscissa. The shaded circles and squares show the result from the monthly mean and annual mean data.

that while all models have $\lambda < 0$ for both forced and unforced calculations (the zero axes are on the right and top edges of the Fig. 2) several models would suggest λ>-0.3 W m^{-2} from the inter-annual variability (λ_{SHORT}) suggesting a very high CS (>12K) whereas none of the models simulate such a large climate sensitivity in response to external forcing. In light of the poor correlation between the inter-model spread in forced CS and λ deduced from inter-annual variability (in the same model), the covariance of RAD_{TOA} and T_S over the satellite era provide almost no constraint on Earth's CS; climate models with comparable inter-annual covariability of T_S and RAD_{TOA} shown by the shaded orange domain (1σ of the observational uncertainty) have a wide range λ_{LONG} values with corresponding climate sensitivities that vary by a factor of four.

The time dependence of λ_{SHORT} and discrepancy between λ_{SHORT} and λ_{LONG} in GCMs suggest one or more underlying assumptions of estimating CS from month-to-month variability have been violated:

- **1.) Time dependence of radiative feedbacks.** The physics that relate surface T_S anomalies to RAD_{TOA} differ between the short term variability and long-term response. Possible causes include (i) differences in the vertical structure of atmospheric temperature changes between month-to-month variability and the long term temperature response (*Chung et al.*, 2012) resulting in different lapse-rate, water vapor and/or cloud feedbacks and (ii) differences in the regional pattern of surface temperature anomalies between the short and long-term responses leading to differing global mean λ (*Feldl and Roe*, 2013) even if the local radiative feedbacks are linear and unchanged (*Armour et al.*, 2013).
- **2.) The regression coefficient between RAD_{TOA} and T_S does not isolate climate feedbacks.** Consider a simplified version of Eq. 1 in which there is no forcing (F=0) and λ is assumed to be time invariant: $RAD_{TOA} = \lambda T_S + \eta_{RAD}$. Given that very little of the RAD_{TOA} variance is explained by the linear fit to T_S in Fig. 1 (R^2 =0.08), we know that the non-

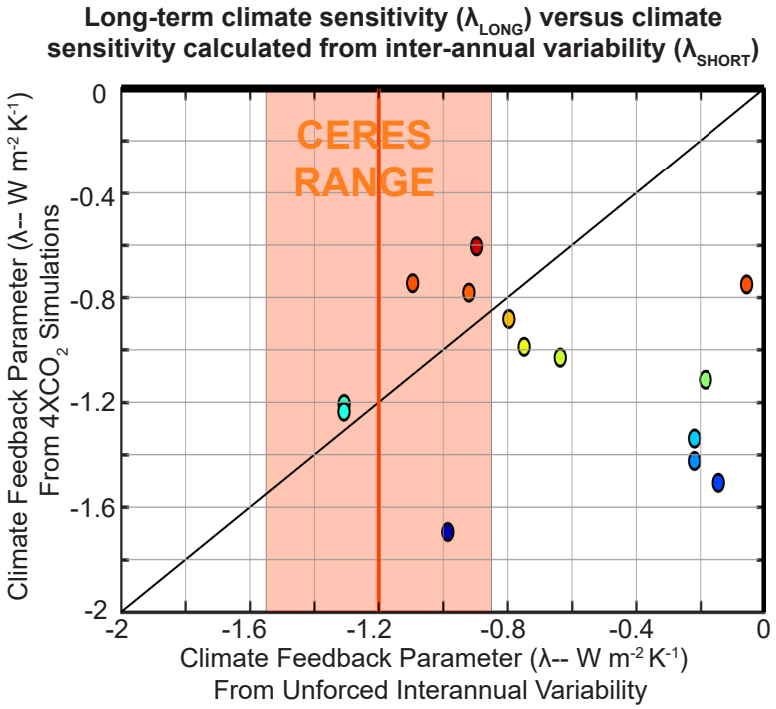

Figure 2: Scatter plot of the global climate feedback parameter (λ in W m^{-2} K^{-1}) calculated from the regression between inter-annual variability in global mean RAD_{TOA} and T_S (λ_{SHORT} – abscissa) versus that calculated from the response to an instantaneous CO_2 quadrupling (λ_{LONG} – ordinate). Each circle represents a different climate model in the suite of CMIP5 coupled models and is color coded according to its long-term climate sensitivity (red/blue models have more/less global warming). The 1:1 line is shown in black. The vertical orange line represents the observational estimate of λ_{SHORT} and its uncertainty (1σ is shaded) calculated from the forcing adjusted month-to-month variability in CERES observations (*Donohoe et al.*, 2014).

feedback radiative variability (η_{RAD}) is substantial. If the noise is truly random with respect to T_S, the regression coefficient between RAD_{TOA} and T_S is not impacted by η_{RAD} and λ can be estimated by the regression coefficient. However, if η_{RAD} is correlated with T_S, as we would expect if some of the global mean surface temperature variability was a result of radiative anomalies, then λ **can not be calculated directly from the regression coefficient between RAD_{TOA} and T_S**.

The goal of the proposed work is to develop and evaluate and define methodologies for removing the above biases from the calculation of long-term CS from short-term variability. If successful, these method will lead to improved observational estimates of climate sensitivity from the existing satellite record.

3 Proposed work

The end goal of the proposed work is to use the spatio-temporal relationship between the CERES satellite record of RAD_{TOA} and observational records of T_S over the relatively short observational period to estimate Earth's CS. This strategy is attractive because the CERES instruments were designed to provide accurate measurements of the short-term (month-to-month) variability in RAD_{TOA} despite the large absolute uncertainties (*Kato et al.*, 2006). Thus, despite our inability to close the TOA radiation budget in the satellite observations (*Trenberth et al.*, 2014) and directly calculate the energy imbalance responsible for global warming (RAD_{TOA}), we can potentially use the co-variability of T_S and RAD_{TOA} over the now 16 years of data – over which there is a small trend and large year-to-year variability– to calculate λ. We have already seen that the linear regression between RAD_{TOA} and T_S (λ_{SHORT}) is highly timescale dependent (Fig. 1) and does not accurately predict long-term CS (Fig. 2). The primary task of the proposed work is, therefore,

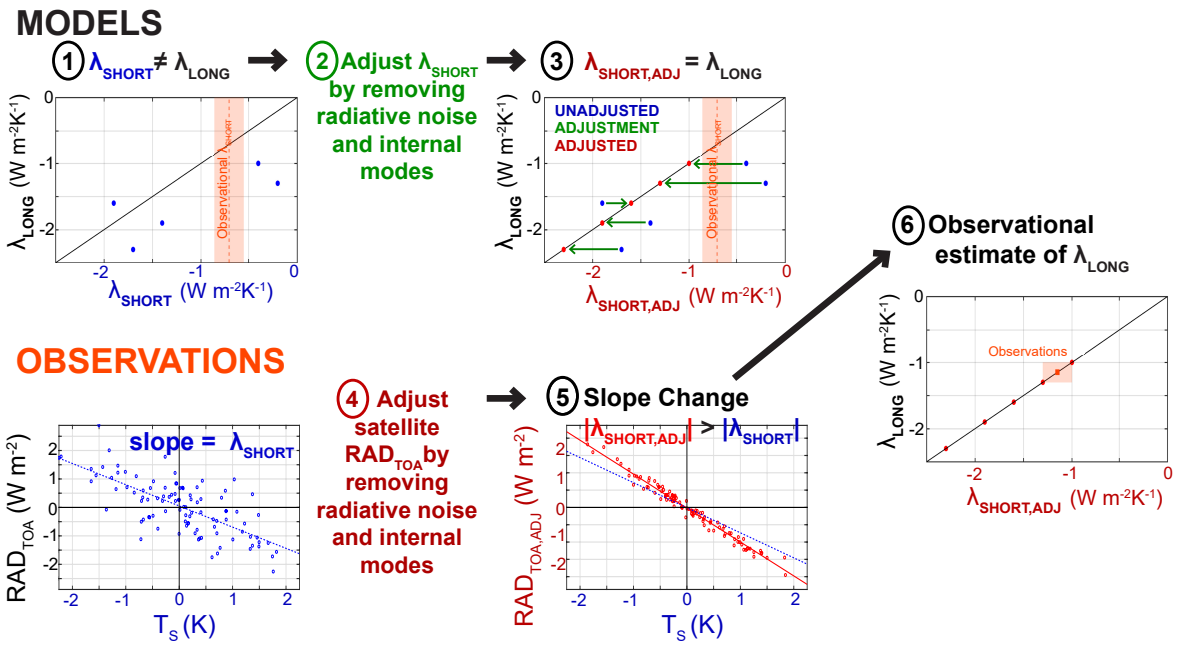

Figure 3: Flow chart of proposed work. Simulations of month-to-month variability and long-term response to greenhouse forcing in CMIP5 GCMs will be used to develop a method for calculating CS from short records of global energy imbalance (via adjustments for internal modes and radiative noise – step 2). The same method will then be applied to the satellite observations to give an improved observational estimate of climate sensitivity (shaded orange box in step 6).

to move beyond simple linear regression and develop a more advanced method for accurately calculating λ_{LONG} from short-term variability that also utilizes the spatio-temporal structure, lagged relationships and coherence between RAD_{TOA}. We will use the CMIP5 multi-model ensemble – where simulations of the both the short-term variability of RAD_{TOA} and long-term response to greenhouse forcing are available– as a training set to develop an adjustment method for calculating λ_{LONG} from short-term variability ($\lambda_{SHORT,ADJ}$ – step 2,3 of schematic flow chart in Fig. 3). We will then apply this (optimized) methodology to the observed satellite record to calculate an improved observational estimate of long-term CS (steps 4-6).

There are several complicating factors in calculating λ from inter-annual variability where the statistical relationship between T_S and RAD_{TOA} may represent processes beyond radiative feedbacks. For instance, if the RAD_{TOA} anomalies that are associated with radiative noise in Eq.1 (η_{RAD}) are correlated with T_S, the linear relationship between T_S and RAD_{TOA} will include the influence of this noise on the estimation of λ. We argue below that this influence is systematic. In the CERES observations, the majority ($\approx 80\%$) of the inter-annual (and monthly) variability in global mean TOA_{RAD} is not explained by forcing and feedbacks but, rather, is speculated to result from anomalies in the atmospheric circulation (*Trenberth et al.*, 2015). Whether the atmospheric variability that gives rise to RAD_{TOA} anomalies is truly random (synoptic) noise or represents a large scale pattern of variability is unclear. More importantly, how these patterns/modes of RAD_{TOA} anomalies that are not associated with climate feedbacks (i.e. not caused by changes in T_S) are potentially related to T_S both physically and statistically (and thus project onto the calculation of λ from inter-annual variability) is unknown and is the focus of this proposal.

We elaborate on the details of the theoretical models and analysis we will pursue to develop a method for calculating CS from short-term variability.

3.1 Internal modes of radiative variability

Internal modes of climate variability may have non-zero global mean T_S and RAD_{TOA} and, therefore, potentially dominate both the variability and covariability of global mean T_S and RAD_{TOA} at the inter-annual timescale. These modes are often characterized by changes in atmospheric circulation where the radiation changes are not a consequence of coupling to the surface but, rather, are due to cloud and humidity changes caused directly by the circulation change. For example, El Nino is associated with increased global mean T_S and a zonal shift in the Walker circulation which has a large impact on RAD_{TOA} in the tropics and globally that are not directly caused by changes in global T_S. As such, the mode of variability may have an associated global λ that is not representative of the long term radiative response to global warming.

We will use empirical orthogonal function analysis to identify the modes of RAD_{TOA} in the PI coupled model simulations, the frequency of the patterns of variability, the consistency of the dominant modes of variability across models and their imprint on global mean RAD_{TOA}. Specifically, we will quantify the λ value implied by the global mean of the mode of radiation variability and that of the associated T_S anomaly? For example, if a given mode of radiative variability explained the entirety of the global RAD_{TOA} variability, the λ calculated from inter-annual variability would simply be the ratio of the global mean RAD_{TOA} and the associated T_S pattern in the mode. If multiple modes contribute to the RAD_{TOA} variability, then the λ calculated from the inter-annual variability can be thought of as the variance explained weighted average of the λ implied by each mode. We will use this methodology to understand why the inter-annual variability of T_S and RAD_{TOA} departs from that expected from the radiative feedbacks alone in Fig. 2; can the λ implied (and variance explained) by the dominant mode of RAD_{TOA} and its difference between models explain the departure of the models from the 1:1 line? In other words, can removing dynamical modes of radiative variability from the observational record isolate surface temperature radiative feedbacks and get us toward an observational estimate of λ that is more representative of climate sensitivity?

The removal of dynamical modes from the inter-annual RAD_{TOA} variability hinges critically on our ability to distinguish and separate dynamical radiative modes from radiative anomalies associated with patterns of T_S variability via genuine radiative feedbacks. To do so, we will look at the vertical structure of the atmospheric temperature, specific humidity, cloud cover and atmospheric circulation anomalies that accompany the radiative variability. Here, we will be looking for RAD_{TOA} anomalies that are not linked to local T_S changes and the associated climate feedbacks but, rather, result from changes in atmospheric circulation. Temperature changes that are amplified aloft, specific humidity changes not associated with local temperature changes (i.e. changes in relative humidity) and translating patterns of clouds that are associated with and co-located with changes in the atmospheric circulation are all tell tale signs of dynamical modes of variability. We can also approximate the RAD_{TOA} due to surface radiative feedbacks from the convolution of radiative kernels (*Soden and Held*, 2006; *Shell et al.*, 2008) and the T_S structure associated with the radiative mode (assuming a vertically uniform temperature change to the tropopause and fixed relative humidity). The discordance between this prediction and the actual climate model RAD_{TOA} output will be used as a more formal evaluation of the imprint of dynamics on radiative modes. After identifying dynamical radiative modes, we will then ask if removing these dynamical modes of

RAD_{TOA} (and their associated T_S) results in a adjusted λ from short-term variability ($\lambda_{SHORT,ADJ}$) that more closely estimates λ_{LONG} in the same model.

Alternative to the EOF method, we can formally remove dynamical modes from RAD_{TOA} by a partial least squares regression between sea level pressure and RAD_{TOA}. This technique was recently used to remove the contribution of dynamics to T_S variability (*Smoliak et al.*, 2015). We will first perform this analysis in the PI coupled climate models where we have long records, internally consistent variables and knowledge of λ_{LONG} from the forced ($4\times CO_2$) experiments. We will ask how long of a record and with what observational certainty we would need to remove dynamical modes from the observed satellite record of RAD_{TOA} and if these techniques can result in an improved estimate of λ over the relatively short satellite record. We will then extend this methodology to the observational record where we will use the reanalyses of atmospheric fields (NCEP and ERA *Kalnay et al.*, 1996; *Dee et al.*, 2011) in conjunction with the CERES data to isolate and remove dynamical modes from the RAD_{TOA} record to derive an improved observational estimate of climate sensitivity from inter-annual variability.

3.2 Conflation of radiative forcing and feedback, timescale dependence and lead/lag relationship between T_S and TOA radiation

While the formulation of Eq. 1 assumes that RAD_{TOA} anomalies are caused by radiative feedbacks initiated by T_S anomalies, a substantial fraction of TOA radiative variability (80% in CERES) is not explained by surface radiative feedbacks. This radiative noise initiates surface heating and T_S anomalies and there is a potential to confuse the impact of RAD_{TOA} on T_S with the impact of T_S on RAD_{TOA} (i.e. radiative feedbacks). The surface temperature tendency resulting from a non-feedback (i.e. noise) radiative anomaly obeys:

$$C\frac{dT_S^{RAD}}{dt} = \eta_{RAD}(t) + F + \lambda T_S^{RAD}, \tag{4}$$

where C is the effective heat capacity of the climate system and η_{RAD} is the RAD_{TOA} noise that is due to internal radiative processes (not associated with external forcing or radiative feedbacks). T_S^{RAD} is the portion of T_S that is forced by the radiation. T_S variability can also be initiated by non-radiative processes (η_{OCE} in W m^{-2}) primarily resulting from changes in ocean circulation and/or heat content:

$$C\frac{dT_S^{OCE}}{dt} = \eta_{OCE}(t) + \lambda T_S^{OCE}. \tag{5}$$

The total surface temperature is the sum of the component contributions forced by radiative noise (η_{RAD}) and internal ocean processes (η_{OCE}):

$$T_S = T_S^{RAD} + T_S^{OCE}. \tag{6}$$

A key question is, how do radiative noise (η_{RAD}) and internal ocean dynamics (η_{OCE}) impact the estimation of λ from unforced variability (F=0) and is this impact random or systematic? Answering these questions will go a long way toward explaining the departure from the 1:1 line in Fig. 2. If there was no radiative noise (η_{RAD} = 0), T_S would be determined entirely by Eq. 5 and the resulting RAD_{TOA} would be perfectly correlated with and in phase with T_S resulting in an exact

estimation of λ from the covariability of RAD_{TOA} and T_S. However, if the radiative noise forces surface heating, that radiative noise is expected to project onto T_S and, thus, will bias the estimation of λ toward a more positive value (consistent with the model bias seen in Fig. 2). Consider, momentarily, the T_S^{RAD} resulting from radiative noise in Eq. 4 with no radiative damping ($\lambda = 0$). The resulting T_S^{RAD} would be in quadrature phase with the radiative noise (η_{RAD}) and, hence, the noise would have no impact on the calculation of λ. However, if the system was damped ($\lambda < 0$) by a genuine radiative feedback (λ) then the resulting T_S^{RAD} still lags the radiative noise but by less than 90°. The resulting phase lag (Θ) of the T_S^{RAD} relative to the radiative noise (η_{RAD}) is given by

$$\Theta(f) = tan^{-1}(\frac{fC}{-\lambda}) \tag{7}$$

where f is the angular frequency of the noise (*Donohoe and Battisti*, 2013). For $\Theta < 90°$, some portion of η_{RAD} is in phase with T_S^{RAD} and, therefore, radiative noise projects onto the calculated λ (*Spencer and Braswell*, 2010); the RAD_{TOA} that is in phase with T_S includes both the feedback (λT_S) that we wish to diagnose and a sub-component ($\propto \cos(\Theta)$) of the noise (η_{RAD}). We propose using the phase relationship in Eq. 7 and variance RAD_{TOA} explained by T_S as an additional constraint for separating the radiative noise from the feedback processes.

As an example, we examine the phase and amplitude relationship between T_S and RAD_{TOA} anomalies in 500 year PI simulation in one of the CMIP5 models (we randomly chose ACCESS1.0 since it was alphabetically first). Fig. 4 shows the lagged regression coefficients between monthly T_S and RAD_{TOA} after first applying a low pass filer with one year cutoff, to emphasize the relationship at lower frequencies. We start our analysis by pursuing the hypothesis that the radiative noise is primarily due to cloud variability resulting in changes in the net solar radiation at TOA (hereafter absorbed solar radiation, ASR). For this reason, TOA radiation is divided into anomalies in ASR (red lines in Fig. 4) and outgoing longwave radiation (OLR – green lines). A "typical" 1K global mean T_S anomaly is preceded (positive y-axis values) by a positive ASR anomaly with energy input to the system peaking 4 months before the surface temperature anomaly at +1.4 W m^{-2}. In contrast, the OLR anomaly is negative and peaks concurrent to the T_S anomaly– as would be expected of the Planck feedback– and implies a longwave feedback of -1.6 W $m^{-2}K^{-1}$. The OLR and ASR feedback parameters (λ_{OLR} and λ_{ASR}) derived from the 4×CO_2 simulation (in ACCESS1.0) via the method of *Forster and Taylor* (2006) are -1.5 and +0.8 W m^{-2} respectively and are shown by the dashed, horizontal lines. The zero lag between T_S and OLR and the near correspondence between the inter-annual regression coefficient and λ_{OLR} suggests that inter-annual OLR anomalies are primarily due to radiative feedbacks associated with the T_S anomaly. In contrast, the phase lead of ASR on T_S suggests that ASR is (at least partly) forcing T_S. Furthermore, the inequality of the lag zero regression coefficient between ASR and T_S and λ_{ASR} (c.f. the solid and dashed red lines) suggests that some portion of the ASR noise is projecting onto the T_S variability and, thus, biasing the feedback calculated from inter-annual variability.

The separation of RAD_{TOA} into ASR and OLR used in the previous paragraph does not adequately separate the forcing and feedback because: a.) the radiative noise initiated by clouds or otherwise impacts OLR alongside ASR and b.) radiative feedbacks impact ASR (through surface albedo feedback, solar absorption by water vapor and cloud changes *Bony et al.*, 2006; *Donohoe et al.*, 2014) alongside OLR. We speculate that the promising initial result of recovering λ_{OLR} from the inter-annual variability and the phase lead of ASR likely results from the noise being dominated by ASR and the feedback being dominated by OLR, at least in the model considered here.

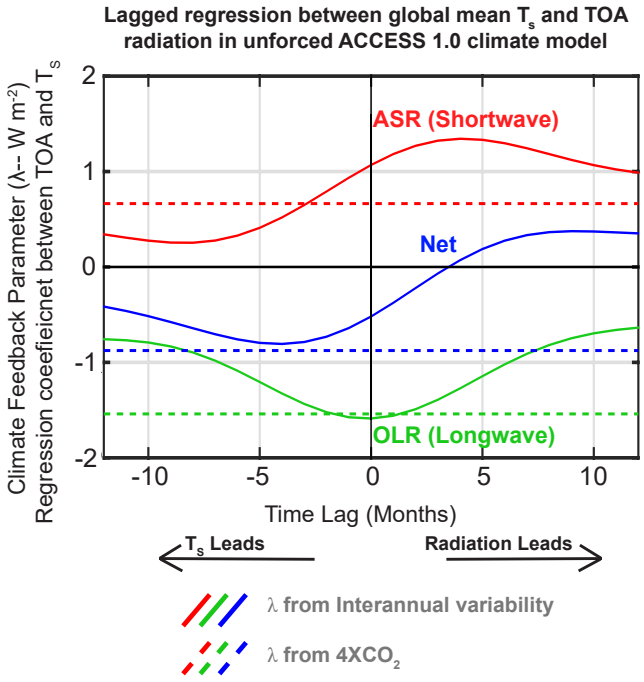

Figure 4: Lagged regressions between global mean RAD_{TOA} and T_S in a 500 year pre-industrial simulation in the CSIRO ACCESS1.0 model. The monthly mean data have been low-pass filtered using a cutoff period of 1 year. Positive lags correspond to radiation leading T_S. The net TOA radiation (blue) has been divided into shortwave (red) and longwave (green) components all defined as positive when into the system. The dashed horizontal lines represent the λ values calculated from the response to $4\times\mathrm{CO}_2$ in the same model.

We need not rely on this assumption to make progress on the problem. Instead, we will analyze the frequency dependence of the relationship between T_S and RAD_{TOA} focusing on the regression coefficients (λ implied from internal variability), phase relationships, and fraction of variance of TOA_{RAD} explained by T_S. The solutions to Eqs. 1 and 4-7 provide predictive equations for four statistical quantities that can be calculated from observations over the satellite era in terms of four unknown variables:

- **Statistical metrics with predictive equations**–1. Variance in T_S, 2. Variance in RAD_{TOA}, 3. Correlation between T_S and RAD_{TOA} (fraction of RAD_{TOA} explained by T_S) and 4. Phase lag between T_S and RAD_{TOA} (phase lag of optimal correlation).
- **Unknown variables**–1.Feedback parameter (λ), 2. Heat Capacity (C), 3. Radiative noise (η_{RAD}) and 4. Noise of internal ocean/surface processes (η_{OCE}).

The above system of equations can be uniquely solved resulting in a quantification of λ and an estimation of the impact of random radiative noise on the regression coefficient between T_S and RAD_{TOA}. Furthermore, if the heat capacity is a constant, the system of equations can be solved uniquely at each frequency. Thus, spectrally decomposing RAD_{TOA} and T_S via a Fourier decomposition potentially results in approximately 90 estimates of λ for the 15 years of CERES data (number of months divided by 2). We will use multitaper spectral techniques (*Ghil et al.*, 2002) to combine multiple spectral representations resulting in more robust signals of the statistical relationships between T_S and RAD_{TOA} in broad spectral bands and the underlying physics. We will first test this methodology in the CMIP5 PI simulations. Ideally, this technique will produce λ values that are frequency independent and agree with the λ calculated from the $4\times\mathrm{CO}_2$ simulations in the same model. We will then apply this technique to the statistical relationships seen between RAD_{TOA} and T_S in the observational record to derive an observational estimate of λ.

The observational calculations will be performed with RAD_{TOA} data from CERES in conjunc-

tion with three different sets of temperature data: 1. the National Centers for Environment Prediction (NCEP) reanalysis surface air temperature (*Kalnay et al.*, 1996), 2. the Goddard Institute for Space Studies Surface Temperature Analysis (GISTEMP) (*Hansen et al.*, 1999) and 3. Cowtan and Way's (*Cowtan and Way*, 2014) adaptation of the Climactic Research Unit of the UK Met Office's Hadley Center (*Morice et al.*, 2012) surface temperature (version 4).

One complicating factor is that the heat capacity (C) is time scale dependent (*Crowley and North*, 1988; *Held et al.*, 2010; *Donohoe et al.*, 2014) due to energy perturbations penetrating deeper into the ocean with time. The spectral technique outlined above potentially overcomes this issue because, provided C is function of frequency only, the set of equations can be applied to each spectral band independently with C representing the (scalar) heat capacity averaged over the frequency band. We can also estimate the heat capacity in climate models by way of the time series analysis of energy content in the climate system and surface temperature (*Donohoe et al.*, 2014). This independent measure of C as a function of frequency will allow us to asses if the our calculation of C from RAD_{TOA} and T_S alone is contaminating our results and if introducing observational ocean heat content data (*Antonov et al.*, 1998; *Levitus et al.*, 2000) would improve our observational estimates of CS.

An alternative approach to the mutual cause-and-effect theoretical relationship between T_S and RAD_{TOA} outlined above is to reverse engineer a methodology for calculating λ from inter-annual variability in climate models where we know the target λ value from the $4\times\mathrm{CO}_2$ simulations. What adjustments and/or filtering of the inter-annual data allows us to best replicate the λ found in the $4\times\mathrm{CO}_2$ simulations in the same model? We will initiate our analysis with a spectral analysis of the frequency dependence of lag zero regression coefficient between T_S and RAD_{TOA}. We expect that the true feedback (λ) is frequency independent so we can use the discordance between the regression coefficient and λ calculated from $4\times\mathrm{CO}_2$ in the same model to pinpoint what frequencies most bias the estimation of λ from internal variability. Would improved estimates of climate sensitivity come from looking at low or high pass filtered internal variability? While intuition suggest that averages over longer periods would be beneficial, Eq. 7 demonstrates that the radiative noise (η_{RAD}) and resulting temperature response (T_S^{RAD}) come closer into phase for longer periods which suggests that low frequency variability is poorly suited for estimating λ. Indeed, our initial analysis finds that removing low frequency variability (periods > 1 year) from T_S and RAD_{TOA} results in a regression coefficients that are in closer agreement with λ from $4\times\mathrm{CO}_2$ experiments and also do not show the same lead/lag relationships shown in Fig. 4. We will use the CMIP5 ensemble to develop a "best" method for estimating λ where "best" is defined by minimizing the ensemble mean distance from the 1:1 line (corresponding to an equality of inter-annual and long term feedbacks) in Fig. 2. We will then use this methodology to calculate an improved estimate of λ in the observations. 16 year sub-samples of the 500 year long PI simulations will be used to assess the error bounds on the λ estimates due to the limited length of the satellite record and how much those estimates will improve if the current observational is maintained into the future. We note that while there is no external forcing in the PI simulations, external forcing does contribute a non-trivial amount of variability to RAD_{TOA} over the satellite record due to trends in well mixed greenhouse gases (e.g. CO_2, CH_4 and $\mathrm{N}_2\mathrm{O}$) and aerosols. We will use updated versions of the same forcing corrections applied by *Donohoe et al.* (2014) that were based on the measurements and radiative transfer calculations of *Solomon et al.* (2011); *Hansen* (1992); *Masarie* (1995).

3.3 Local versus global feedbacks; the role of dynamics, surface fluxes and thermal stratification

Local RAD_{TOA} responds to local T_S via surface radiative feedbacks as well as changes in the thermal stratification, humidity and cloud cover induced by both the lateral energy flux convergence in the atmosphere and surface energy fluxes. Similar to the global mean TOA radiative balance formulated in Eq. 1, the local RAD_{TOA} anomaly can be expressed as

$$RAD_{TOA}(X,Y,t) = F(X,Y,t) + \lambda_{LOC}(X,Y)T_S(X,Y,t) + \eta_{RAD}(X,Y,t), \quad (8)$$

where λ_{LOC} is the local climate feedback parameter defined as the change is TOA radiation that results from a local T_S change via radiative feedbacks (units of W m^{-2} K^{-1}) and we have explicitly shown the dependence of the variables on longitude (X) and latitude (Y). λ_{LOC} in climate models (diagnosed via radiative kernels) is overwhelmingly negative due to the dominance of the nearly spatially uniform negative Planck. However, there are significant spatial variations in λ_{LOC} due to spatial inhomogeneities in the cloud, surface albedo and water vapor feedbacks (*Armour et al.*, 2013). In contrast, recent attempts to diagnose λ_{LOC} from the inter-annual covariability of RAD_{TOA} and T_S found λ_{LOC} to be overwhelmingly positive in both observations (*Trenberth et al.*, 2015) and models. *Brown et al.* (2015) demonstrated that implied positive λ_{LOC} in models results from changes in high latitude surface albedo, mid-latitude clouds and tropical humidity that are initiated by lateral atmospheric energy fluxes (i.e. atmospheric dynamics) and surface energy fluxes (i.e. ocean dynamics) that covary with local T_S. In this case, both RAD_{TOA} and T_S are responding to an external variable (circulation changes) and the covariance between T_S is capturing the sum of three processes: 1. The surface temperature radiative feedback ($\lambda_{LOC}T_S$); 2. Radiative noise forcing T_S changes; and 3. The mutual dependence of RAD_{TOA} and T_S on an external variable. We desire an evaluation of process 1 from the inter-annual variability of the satellite record but anticipate (and see from the work of *Trenberth et al.* (2015) and *Brown et al.* (2015)) that processes 2 and 3 will contaminate the diagnosis of λ_{LOC} from the local temporal covariance of T_S and RAD_{TOA}.

Both the methodologies outlined in the previous two subsections will be applied at the local scale in order to develop a methodology for evaluating λ_{LOC} from the satellite record. First, the dynamical modes of RAD_{TOA} variability and their associated T_S will be removed from the record via the EOF and/or partial least squares regressions methods outlined in Section 3.1. Next, the impact of local radiative noise (η_{RAD}) on local T_S and its potential contamination on the calculation of λ_{LOC} will be evaluated and removed via the methodology discussed in Section 3.2. The combination of these techniques will remove both the dynamic variability of RAD_{TOA} and the impact of radiative noise forcing the local surface temperature from the calculation of λ_{LOC}. We will first perform these calculation in climate models where we can compare the λ_{LOC} evaluated from the inter-annual variability to that calculated from both radiative kernels (*Soden and Held*, 2006; *Shell et al.*, 2008) and the response to external forcing via the method of *Gregory et al.* (2004) applied locally.

What is the value of determining λ_{LOC}? Global climate sensitivity is a metric of how efficiently the climate system exports energy radiatively to space as the surface warms and is intuitively a consequence of the same physics that determine λ_{LOC}. However, global mean climate sensitivity is not simply the spatial average of regional climate sensitivity implied by λ_{LOC} nor is the regional climate response to forcing determined solely by local radiative feedbacks (λ_{LOC}). The following example illustrates these points. Say we apply spatially uniform forcing to two adjacent regions of

the climate system: **Region 1** with a large magnitude negative λ_{LOC} and **Region 2** with $\lambda_{LOC} = 0$. Region 2 does not lose energy via radiation as it warms and, if isolated from the rest of the climate system would heat up indefinitely. However, as region 2 heats up, it will flux energy to region 1 which can then export energy to space via radiative feedbacks. There are two essential lessons to the above example; in the long-term response to external forcing, the global climate sensitivity is determined by the λ_{LOC} in the regions that are most efficient at exporting radiation to space (region 1) and the ability of the dynamics to move energy from region 2 to region 1 (*Pierrehumbert*, 1995). Overall, the atmosphere and or ocean must move energy up the λ_{LOC} gradient in order to satisfy both global and local energy constraints (*Roe et al.*, 2015). Thus, an observational determination of λ_{LOC} and its uncertainty is a much more powerful constraint for future climate predictions than an evaluation of global λ for three reasons: 1. it pinpoints which regions and dynamical processes contribute most to our uncertainty in global climate sensitivity and potentially informs our focus of future observational and modeling endeavors; 2. it predicts how atmospheric circulations will adjust to external forcing; and 3. it predicts the spatial pattern of global warming (*Roe et al.*, 2015).

3.4 Designing observational programs to optimize the estimation of global climate sensitivity

How can future observational programs be designed and prolonged to make more accurate evaluations of CS? The combination of long control simulations and known long-term CS in the ensemble of CMIP5 models provides a near perfect opportunity to assess how accurately we can estimate CS from finite records of month-to-month variability via the methodology developed in the proposed work. We will apply our optimal method for calculating $\lambda_{SHORT,ADJ}$ to subsets of control simulations of equal length to the satellite record to ask how accurately the calculated $\lambda_{SHORT,ADJ}$ matches λ_{LONG} (response to $4XCO_2$) in the same model and how wide the distribution of $\lambda_{SHORT,ADJ}$ is given a relatively short observational record. We can then increase the length of the subsets used to calculate $\lambda_{SHORT,ADJ}$ to answer how much we can improve the estimate of CS by sustaining a consistent satellite observation network in future decades by analyzing how much the distribution of $\lambda_{SHORT,ADJ}$ narrows and converges to CS across the subset of anaylses. Furthermore, we can ask how having additional/increased accuracy of observational fields would improve our methodology for removing radiative noise (associated with internal modes) from the calculation of $\lambda_{SHORT,ADJ}$ by excluding/adding noise to model fields used to calculate $\lambda_{SHORT,ADJ}$. In this sense, subsets of the CMIP5 models will act as observing system simulation experiments for the observational estimation of CS.

4 Relevance to NASA Goals

The proposed work will use *"space based measurements to provide information not available by other means"*, by utilizing the inter-annual variability of CERES measurements, to derive an improved observational estimate of Earth's climate sensitivity that will directly *"improve our capability for predicting its [Earth's] future evolution"* and *"advance the understanding of changes in the Earth's radiation balance"*. Furthermore, our analysis of the inter-annual variability in global mean energy budgets will directly *"characterize its [Earth's] properties on a broad range of spatial and*

temporal scales, to understand the naturally occurring and human induced processes that drive" variability .

5 Working Timeline

We emphasize that Dr. Donohoe (PI) currently holds a post-doctoral associate position. It is expected that he will transition to a research scientist position in the upcoming year if this proposal is successful. The working timeline below represents 4 months of work per year for the PI. The observational analysis and CMIP5 model output analysis described in this proposal will be performed by the the PI and will guide collaborative modeling efforts by two different collaborators (not financially supported under the proposed budget): Professor Piers Forster (University of Leeds, U.K. – radiative transfer calculations to support interpretation of dynamical modes) and Professor Kyle Armour (Department of Oceanography, University of Washington– assessment of internal radiative variability using radiative kernels and idealized "aquaplanet" simulations).

- **Year one–Climate sensitivity from time series and spectral analysis of unforced covariability of T_S and RAD_{TOA}**
  1. Decomposing the mutual cause-and-effect relationship between global mean T_S and RAD_{TOA} into radiative feedback ($T_S \rightarrow RAD_{TOA}$) and radiative noise forcing T_S ($RAD_{TOA} \rightarrow T_S$) to derive estimates of λ from inter-annual variability in pre-industrial simulations.
  2. Reverse engineering a method for calculating climate sensitivity from inter-annual variability. Analyze the covariability of T_S and RAD_{TOA} and its comparison to the climate feedbacks caused by external forcing in the same model to determine what spectral bands and adjustments give the "best" estimates of climate sensitivity from inter-annual variability
  3. Apply above methodologies to (forcing adjusted, inter-annual) CERES record of RAD_{TOA} and reanalyses of surface temperature.
- **Year two –Internal modes of radiative variability**
  1. Calculate empirical orthogonal functions of unforced radiative variability in pre-industrial model simulations and their implied λ
  2. Use analysis of atmospheric circulation and thermal structure to identify and remove dynamic modes
  3. Repeat and compare with removal of dynamical modes via multiple least square regressions and identify if removing such modes from inter-annual variability results in a better estimate of climate sensitivity
  4. Apply same methodology to satellite record and establish observed climate system with error bounds based on discordance between the dynamically adjusted inter-annual variability and climate sensitivity in models and the limited length of satellite observations
- **Year three – Spatial patterns of climate feedbacks**
  1. Remove the local influence of dynamic variability and the covariance of radiative noise and T_S from PI simulations to estimate λ_{LOC} in models and compare to that derived from radiative kernels and forced experiments
  2. Apply to satellite record to identify spatial patterns of feedbacks

6 References

References

Antonov, J., S. Levitus, T. Boyer, M. Conkright, T. OBrien, and C. Stephens (1998), World ocean atlas 1998 vol. 1: Temperature of the atlantic ocean, *NOAA Atlas NESDIS*, *27*, 166 pp.

Armour, K., and G. Roe (2011), Climate commitment in an uncertain world, *Geophys. Res. Lett.*, *38*, doi:10.1029/2010GL045850.

Armour, K., C. Bitz, and G. Roe (2013), Time-varying climate sensitivity from regional feedbacks., *J. Climate*, *26*, 4518–4534.

Battisti, D., and R. Naylor (2009), Historical warnings of future food insecurity with unprecedented seasonal heat, *Science*, *323*(5911), 240–244.

Bony, S., et al. (2006), How well do we understand climate change feedback processes?, *J. Climate*, *19*, 3345–3482.

Brown, P., W. Li, J. Jiang, and H. Su (2015), The toa energy balance and its opposite relationship with surface temperature anomalies at local and global scales, *J. Climate*, p. In Press.

Caldwell, P., C. Bretherton, M. Zelinake, S. Klein, B. Santer, and B. Sanderson (2015), Statistical significance of climate sensitivity predictors obtained by data mining, *Geophys. Res. Lett.*, *41*, 1803–1808, doi:10.1002/2014GL059205.

Chung, E., B. Soden, and B. Sohn (2010), Revisiting the determination of climate sensitivity from relationships between surface temperature and radiative fluxes, *Geophys. Res. Lett.*, *37*(10), doi:10.1029/2010GL043051.

Chung, E., B. Soden, and A. Clement (2012), Diagnosing climate feedbacks in coupled oceanŰatmosphere models, *Surv. Geophys.*, *33*, doi:10.1007/s10712-012-9187-x.

Cowtan, K., and R. Way (2014), Coverage bias in the hadcrut4 temperature series and its impact on recent temperature trends, *140*(683), 1935–1944.

Crowley, T., and G. North (1988), Abrupt climate change and extinction events in earth history., *Science*, *240*(996), 1002.

Dee, D., et al. (2011), The era-interim reanalysis: configuration and performance of the data assimilation system, *Quart. J. Roy. Meteor. Soc.*, *137*, 553–597.

Dessler, A. (2013), Observations of climate feedbacks over 2000-2010 and comparisons to climate models, *J. Climate*, *26*, 333–342.

Deutsch, C., J. Tewksbury, R. Huey, K. Sheldon, C. Ghalambor, D. Haak, and P. Martin (2008), Impacts of climate warming on terrestrial ectotherms across latitude, *Proc. Nat. Acad. Sci. USA*, *105*(18), 6668–6672.

Donohoe, A., and D. Battisti (2013), The seasonal cycle of atmospheric heating and temperature, *J. Climate*, *26*(14), 4962–4980.

Donohoe, A., K. Armour, A. Pendergrass, and D. Battisti (2014), Shortwave and longwave contributions to global warming under increasing co_2., *Proc. Nat. Acad. Sci. USA*, *111*(47), 16,700–16,705.

Fasullo, J. T., and K. E. Trenberth (2012), A less cloudy future: The role of subtropical subsidence in climate sensitivity., *Science*, *338*(6108), 792–794, doi:10.1126/science.1227465.

Feldl, N., and G. Roe (2013), The nonlinear and nonlocal nature of climate feedbacks., *J. Climate*, *26*, 8289–8304.

Forster, P. (2015), Inference of climate sensitivity from analysis of Earth's energy budget, *rgph*, doi:10.1146/annurev-earth-060614-105156.

Forster, P., and K. Taylor (2006), The climate sensitivity and its components diagnosed from earth radiation budget data, *jcli*, *19*, 39–52.

Forster, P., T. Andrews, P. Good, J. Gregory, L. Jackson, and M. Zelinka (2013), Evaluating adjusted forcing and model spread for historical and future scenarios in the cmip5 generation of climate models, *jgr*, *118*(3), 1139–1150.

Ghil, M., et al. (2002), Advanced spectral methods for climatic time series., *Rev. Geophys.*, *40*, doi:10.1029/2001RG000092.

Gregory, J., and M. Webb (2008), Tropospheric adjustment induces a cloud component in co_2 forcing, *J. Climate*, *21*, 58–71.

Gregory, J. M., W. Ingram, M. Palmer, G. Jones, P. Stott, R. Thorpe, J. Lowe, T. Johns, and K. Williams (2004), A new method for diagnosing radiative forcing and climate sensitivity, *Geophys. Res. Lett.*, *31*, L03,205, doi:10.1029/2003gl018747.

Hansen, J., R. Ruedy, J. Glascoe, and M. Sato (1999), Giss analysis of surface temperature change, *J. Geophys. Res.*, *104*, 30,997–31,022.

Hansen, J. e. a. (1992), Efficacy of climate forcings, *J. Geophys. Res.*, *110*(D18), D18,104.

Held, I., and B. Soden (2006), Robust responses of the hydrological cycle to global warming., *J. Appl. Meteor.*, *19*(21), 5686–5699.

Held, I., M. Winton, K. Takahashi, T. Delworth, F. Zeng, and G. Vallis (2010), Probing the fast and slow components of global warming by returning abruptly to preindustrial forcing, *J. Climate*, *23*, 2418–2427.

Holland, M. M., and C. Bitz (2003), Polar amplification of climate in coupled models., *Climate Dyn.*, *21*, 221–232.

Kalnay, E., et al. (1996), The NCEP/NCAR 40-year reanalysis project., *Bull. Amer. Meteor. Soc.*

Kato, S., N. Loeb, P. Minnis, J. Francis, T. Charlock, D. Rutan, E. Clothiaux, and S. Sun-Mack (2006), Seasonal and interannual variations of top-of-atmosphere irradiance and cloud cover over polar regions derived from ceres data set., *Geophys. Res. Lett.*, *33*, doi:10.1029/2006GL026,685.

Levitus, S., J. Antonov, T. Boyer, and C. Stephens (2000), Anthropogenic warming of earth's climate system, *Science*, *287*(5461), 2225–2229, doi:10.1126/science.287.5461.2225.

Loeb, N. G., B. A. Wielicki, D. R. Doelling, G. L. Smith, D. F. Keyes, S. Kato, N. Manalo-Smith, and T. Wong (2009), Towards optimal closure of the earth's top-of-atmosphere radiation budget., *J. Climate*, *22*, 748–766.

Lu, J., G.Vecchi., and T. Reichler (2007), Expansion of the hadley cell under global warming, *Geophys. Res. Lett.*, *34*(6), doi:10.1029/2006GL028443.

Marvel, K., G. Schmidt, R. Miller, and L. Nazarenko (2015), Implications for climate sensitivity from the response to individual forcings, *Nat. Clim. Chang.*, *6*, 386–389.

Masarie, M. P. T. (1995), Extension and integration of atmospheric carbon dioxide data into a globally consistent measurement record, *J. Geophys. Res.*, *100*, 11,593–11,610.

Morice, C. P., J. Kennedy, N. Rayner, and P. Jones (2012), Quantifying uncertainties in global and regional temperature change using an ensemble of observational estimates: The hadcrut4 dataset, *J. Geophys. Res.*, *117*, D08,101.

Murphy, D., S. Solomon, R. Portmann, K. Rosenlof, and F.P.M. (2009), An observationally based energy balance for the earth since 1950, *J. Geophys. Res.*, *114*, D17,107.

Myhre, G., E. Highwood, K.P.Shine, and F. Stordal (1998), New estimates of radiative forcing due to well mixed greenhouse gases, *Geophys. Res. Lett.*, *25*(14), 2715–2718.

Myhre, G., et al. (2013), *Anthropogenic and Natural Radiative Forcing*, book section 8, p. 659Ű740, Cambridge University Press, doi:10.1017/CBO9781107415324.018.

Nichols, R., and A. Cazenave (2010), Sea-level rise and its impact on coastal zones, *Science*, *328*(5985), 1517–1520.

Oki, T., and S. Kanae (2006), Global hydrological cycles and world water resources, *Science*, *313*(5790), 1068–1072.

Pierrehumbert, R. (1995), Thermostats, radiator fins, and the local runaway greenhouse, *J. Atmos. Sci.*, *52*, 1784–1806.

Rhein, M., et al. (2013), *Observations: Ocean*, book section 3, p. 255Ű316, Cambridge University Press, Cambridge, United Kingdom and New York, NY, USA, doi: 10.1017/CBO9781107415324.010.

Roe, G., N. Feldl, K. Armour, Y.-T. Hwang, and D. Frierson (2015), The remote impacts of climate feedbacks on regional climate predictability., *Nature Geosci.*, *8*, 135–139, doi: 10.1038/ngeo2346.

Shell, K., J. Kiehl, and C. Shields (2008), Using the radiative kernel technique to calculate climate feedbacks in ncar's community atmospheric model., *J. Climate*, *21*, 2269–2282.

Sherwood, S., P. Forster, G. Gregory, S. Bony, B. Stevens, and C. Bretherton (2014), Adjustments in the forcing feedback framework for understanding climate change, *Bull. Amer. Meteor. Soc.*, *96*, 217–228.

Smoliak, B., J. Wallace, P. Lin, and Q. Fu (2015), Dynamical adjustment of the northern hemisphere surface air temperature field: Methodology and application to observations., *J. Climate*, *28*, 1613–1629.

Soden, B., and I. Held (2006), An assessment of climate feedbacks in coupled oceanŰatmosphere models, *J. Climate*, *19*, 3354–3360.

Solomon, S., J. Daniel, R. Neely, J.-P. Vernier, E. Dutton5, and L. Thomason (2011), The persistently variable Şbackgroundt stratospheric aerosol layer and global climate change, *Science*, *333*(6044), 866–870.

Spencer, R., and W. Braswell (2010), On the diagnosis of radiative feedback in the presence of unknown radiative forcing, *J. Geophys. Res.*, *115*(D16109), doi:10.1029/2009JD013371.

Stocker, T., et al. (2013), *Technical Summary*, book section TS, p. 33Ű115, Cambridge University Press, Cambridge, United Kingdom and New York, NY, USA, doi:10.1017/CBO9781107415324.005.

Taylor, K., R. Stouffer, and G. Meehl (2012), An overview of cmip5 and the experiment design., *Bull. Amer. Meteor. Soc.*, *93*, 485–498.

Trenberth, K. E., J. T. Fasullo, C. O'Dell, and T. Wong (2010), Relationships between tropical sea surface temperature and top-of-atmosphere radiation, *Geophys. Res. Lett.*, *37*(3), doi:10.1029/2009GL042314.

Trenberth, K. E., J. Fasullo, and M. Balmaseda (2014), Earths energy imbalance, *J. Climate*, *27*, 3129–3144, doi:10.1175/JCLI-D-13-00294.

Trenberth, K. E., Y. Zhang, J. Fasullo, and S. Taguchi (2015), Climate variability and relationships between top-of-atmosphere radiation and temperatures on earth, *J. Geophys. Res.*, *120*, 3642–3659, doi:10.1002/2014JD022887.

Tsushima, Y., A. AbeOuchi, and S. Manabe (2005), Radiative damping of annual variation in global mean surface temperature: comparison between observed and simulated feedback, *Climate Dyn.*, *24*, 591–597.

Wielicki, B., B. Barkstrom, E. Harrison, R. Lee, G. Smith, and J. Cooper (1996), Clouds and the earth's radiant energy system (CERES): An earth observing system experiment., *Bull. Amer. Meteor. Soc.*, *77*, 853–868.

Yin, J. (2005), A consistent poleward shift of the storm tracks in simulations of 21st century climate, *Geophys. Res. Lett.*, *32*(18), doi:10.1029/2005GL023684.